EUKARYOTIC CELL, Feb. 2005, p. 365–378 Vol. 4, No. 2
1535-9778/05/$08.00+0 doi:10.1128/EC.4.2.365–378.2005

The Heterotrimeric G-Protein Subunits GNG-1 and GNB-1 Form a Gβγ Dimer Required for Normal Female Fertility, Asexual Development, and Gα Protein Levels in *Neurospora crassa*

Svetlana Krystofova and Katherine A. Borkovich*

Department of Plant Pathology, University of California—Riverside, Riverside, California

Received 24 September 2004/Accepted 18 November 2004

We have identified a gene encoding a heterotrimeric G protein γ subunit, *gng-1*, from the filamentous fungus *Neurospora crassa*. *gng-1* possesses a gene structure similar to that of mammalian Gγ genes, consisting of three exons and two introns, with introns present in both the open reading frame and 5′-untranslated region. The GNG-1 amino acid sequence displays high identity to predicted Gγ subunits from other filamentous fungi, including *Giberella zeae*, *Cryphonectria parasitica*, *Trichoderma harzianum*, and *Magnaporthe grisea*. Deletion of *gng-1* leads to developmental defects similar to those previously characterized for Δ*gnb-1* (Gβ) mutants. Δ*gng-1*, Δ*gnb-1*, and Δ*gng-1* Δ*gnb-1* strains conidiate inappropriately in submerged cultures and are female sterile, producing aberrant female reproductive structures. Similar to previous results obtained with Δ*gnb-1* mutants, loss of *gng-1* negatively influences levels of Gα proteins (GNA-1, GNA-2, and GNA-3) in plasma membrane fractions isolated from various tissues of *N. crassa* and leads to a significant reduction in the amount of intracellular cyclic AMP. In addition, we show that GNB-1 is essential for maintenance of normal steady-state levels of GNG-1, suggesting a functional interaction between GNB-1 and GNG-1. Direct evidence for a physical association between GNB-1 and GNG-1 in vivo was provided by coimmunoprecipitation.

G-protein-linked pathways evolved to allow responses to extracellular agonists (hormones, neurotransmitters, odors, chemoattractants, light, and nutrients) in eukaryotic cells, ranging from simpler systems, including yeasts, filamentous fungi, and slime molds, to more complex organisms, such as mammals. The G protein βγ dimer performs numerous roles during the signal transduction process (for reviews, see references 14 and 32), including membrane targeting of the α subunit (23), recognition of receptors (46), activation of downstream effectors (14), and modulation of different proteins affecting signal intensity or duration (47). Multiple isoforms, including 6 Gβ and 12 Gγ subunits, have been identified in mammals (14, 32, 50). In mammals, a major challenge for in vivo identification of Gβγ dimers and establishment of their roles in particular signaling pathways arises from the variety of possible combinations between β and γ subtypes.

In contrast to the situation with mammals, only one Gβ subunit is present in all sequenced fungal genomes (http://www.yeastgenome.org; http://www.genedb.org/genedb/pombe/index.jsp; http://www.broad.mit.edu/annotation/fungi) (27). For the budding yeast *Saccharomyces cerevisiae*, previous studies have indicated that the Ste4p Gβ functions as a positive regulator of the pheromone response in haploid cells by activation of the downstream mitogen-activated protein kinase cascade, leading to cell cycle arrest, shmoo formation, cell fusion, and karyogamy (for reviews, see references 22 and 42). Gpa1p, the Gα protein that interacts with Ste4p, functions as a negative regulator of the pathway. In the fission yeast *Schizosaccharomyces pombe*, the Gβ subunit Git5 is required for glucose sensing and mating through activation of cyclic AMP (cAMP) signaling (45). In the basidiomycete human pathogenic fungus *Cryptococcus neoformans*, deletion of the Gβ subunit gene *GPB-1* results in sterility and defective monokaryotic fruiting (72). Mutation of the Gβ gene *sfaD* from the filamentous fungus *Aspergillus nidulans* leads to hyperactive conidiation (asexual sporulation) and reduced vegetative growth (56). In the chestnut blight pathogen *Cryphonectria parasitica*, disruption of the *cpgb-1* Gβ subunit gene negatively affects virulence, conidiation, pigmentation, and hyphal branching, while stimulating growth on vegetative solid medium (40). In *Magnaporthe grisea*, the causative agent of rice BLAST disease, mutants disrupted in the Gβ subunit *MGB1* exhibit reduced growth and conidiation, defective appressorium formation, and reduced intracellular cAMP levels (51). Loss of *gnb-1* in the filamentous fungus *Neurospora crassa* leads to inappropriate conidiation in submerged culture, altered mass accumulation on solid medium, production of aberrant fertilized female reproductive structures, reduced intracellular cAMP levels, and low levels of all three Gα subunits (80).

Gγ subunits belong to a large family of small proteins consisting of 68 to 75 amino acids with different primary structures in various species (6, 20, 28). All Gγ proteins contain the CaaX box motif at the carboxy terminus that is subject to posttranslational modification, including isoprenylation and subsequent carboxyl methylation (28, 82). This posttranslational modification of Gγ subunits determines the subcellular localization of the Gβγ complex, in that it targets the heterodimer to the plasma membrane (36, 48, 58). The carboxy-terminal modification of Gγ is also necessary for effective interaction of Gβγ with other proteins, including Gα, downstream effectors, and receptors (12).

Only a single Gγ subunit gene has been identified in the yeasts *S. cerevisiae* (*STE18*) and *S. pombe* (*git11*) (45, 76). In *S.*

* Corresponding author. Mailing address: Department of Plant Pathology, 1415 Boyce Hall, 900 University Ave., University of California Riverside, CA 92521. Phone: (951) 827-2753. Fax: (951) 827-4294. E-mail: Katherine.Borkovich@ucr.edu.

TABLE 1. *N. crassa* strains

Strain	Relevant genotype	Comment(s)	Source or reference
74A-OR23-1A (74A)	Wild type, *matA*	FGSC[a] #987	FGSC
74a-OR8-1a (74a)	Wild type, *mata*	FGSC #988	R. L. Weiss (UCLA)
73a	Wild type, *mata*		R. L. Weiss (UCLA)
FGSC #4564	*cyh-1 ad*3B a^{m1}	Helper strain	FGSC
42-8-3	Δ*gnb-1*::*hph*$^+$ *matA*	Δ*gnb-1* homokaryon	80
FGSC #6103	*his-3, matA*	*his-3* targeting strain	FGSC
his3a	*his-3, mata*	FGSC #6103 × 73a progeny	This study
hβJ	Δ*gnb-1*::*hph*$^+$ *his-3 mata*	his-3a × 42-8-3 progeny	This study
5-5-3	Δ*gng-1*::*hph*$^+$ *matA*	Δ*gng-1* homokaryon	This study
5-5-8	Δ*gng-1*::*hph*$^+$ *matA*	Δ*gng-1* homokaryon	This study
5-5-12	Δ*gng-1*::*hph*$^+$ *matA*	Δ*gng-1* homokaryon	This study
FH1[b]	Δ*gnb-1*::*hph*$^+$ *his-3* + *cyh-1 ad*3B, a^{m1}	Heterokaryon of 42-8-3 and FGSC #4564	This study
5-4	Δ*gnb-1*::*hph*$^+$ Δ*gng-1*::*hph*$^+$ *matA*	FH1 × 5-5-3 progeny	This study
113	Δ*gng-1*::*hph*$^+$ *his-3 mata*	5-5-12 × his-3a progeny	This study
113-1	Δ*gng-1*::*hph*$^+$ *gng-1*$^+$::*his-3*$^+$ *mata*	Complemented Δ*gng-1* mutant	This study
5A	Δ*gng-1*::*hph*$^+$ FLAG-*gng-1*$^+$::*his-3*$^+$ *mata*	Strain expressing FLAG-tagged GNG-1	This study

[a] FGSC, Fungal Genetics Stock Center, Kansas City, Mo.
[b] FH1, a forced heterokaryon between the Δ*gnb-1 his-3* (hβJ) strain and the a^{m1} FGSC #4564 helper strain, was crossed to Δ*gng-1* strain 5-5-3. Progeny carry genes from the hβJ and 5-5-3 strain backgrounds only, as the a^{m1} nucleus is not passaged during a cross.

cerevisiae, previous studies have demonstrated that haploid cells of opposite mating type lacking the *STE18* or *STE4* gene are unable to mate (76). Genetic studies indicate that Ste4p binds to Ste18p, and various *ste18* mutations have been isolated that either suppress or enhance phenotypic defects of *ste4* alleles (15, 77). Furthermore, Ste18p has been shown to physically interact with Ste4p (15, 34, 64) and to tether the Gβγ dimer to the plasma membrane (9, 34, 64). Deletion of the *git11* gene in *S. pombe* confers phenotypes associated with defects in the glucose-sensing (cAMP) pathway. Δ*git11* cells are defective in glucose repression of both *fbp1* (encoding fructose-1,6-bisphosphatase) and sexual development, and they resemble cells lacking either *gpa2* Gα or *git5* Gβ (45, 73). Moreover, a physical interaction between Git11p and Git5p has been demonstrated by coimmunoprecipitation (45).

To date, Gγ proteins have not been characterized in any filamentous fungal species. In this study, we present the identification, isolation, and characterization of a predicted Gγ subunit, *gng-1*, from the fungus *N. crassa*. Δ*gng-1* and Δ*gnb-1* Δ*gng-1* mutants were isolated and analyzed for phenotypes during vegetative growth as well as asexual and sexual development. Levels of the three Gα proteins and mRNA levels were analyzed, and intracellular amounts of cAMP were quantitated. Evidence for a physical association between GNG-1 and GNB-1 in vivo was probed using coimmunoprecipitation. Our results indicate that GNG-1 and GNB-1 form a functional Gβγ heterodimer that is essential for normal asexual sporulation and female fertility in *N. crassa*.

MATERIALS AND METHODS

Strain manipulations and media. *Neurospora* strains used in this study are listed in Table 1. Vogel's minimal medium (VM) (70) was used for vegetative growth, while synthetic crossing medium (SCM) (74) was used to induce development of female reproductive structures. Sorbose-containing medium was used to facilitate colony formation on plates (16). If required, hygromycin B (Calbiochem) was added to media at a concentration of 200 μg/ml. Seven-day-old conidia were used to inoculate all cultures. Plasmids were maintained in *Escherichia coli* strain DH5α (33).

Isolation and sequencing of the *gng-1* gene. A Gγ gene was initially identified during homology searches (BLAST) (1) of the *N. crassa* cDNA database at the University of Oklahoma (http://www.genome.ou.edu) using the protein sequence of *S. cerevisiae* Ste18p. Two cDNA clones, b7a10ne and a8h02ne, encoding hypothetical proteins similar to Gγ subunits, were identified. The 1.2-kb insert of a8h02ne was used to screen a BARGEM-7λ genomic library (53). Two positive plaques were obtained and converted to double-stranded plasmids (53), and they were subsequently subjected to Southern analysis using the insert from a8h02ne as a probe. Both cDNA clone a8h02ne and one of the genomic clones (designated #31; insert size, 4.5 kb) were sequenced (Core Sequencing Facility, Department of Microbiology and Molecular Genetics, University of Texas—Houston Medical School). The entire sequence of the cDNA clone a8h02ne and a partial sequence from one of the genomic clones were analyzed. The sequence of the *gng-1* open reading frame (ORF) identified in genomic clone #31 was used to search the *N. crassa* genome database (http://www.broad.mit.edu/annotation/fungi/neurospora) using BLAST searches and was found to correspond to predicted protein NCU00042.1.

The *gng-1* replacement mutation and complementation by *gng-1*$^+$ in *trans*. The *gng-1* ORF is located only 790 bp away from the 3′ end of the insert in genomic clone #31. To make a gene replacement construct, a larger genomic clone (#2231) with an insert size of 6.5 kb was used (see Fig. 2A). The *gng-1* gene was replaced with the *hph* gene encoding hygromycin B phosphotransferase under control of the *A. nidulans trp*C promoter as follows. The *hph* cassette was first removed from pCSN44 (66) using BamHI and SalI and was subsequently cloned into pBlueScript KS+ (Stratagene), generating pSVK5. KpnI and SpeI were used to excise the *hph* fragment from pSVK5; this fragment was then used to replace the portion of the *gng-1* ORF between the KpnI site and the second SpeI site of the genomic clone, yielding pSVK7 (Fig. 2A). pSVK7 contains 2.5 kb of 5′-flanking DNA and 2.4 kb of 3′-flanking DNA extending from the EcoRI to EcoRV sites in the *gng-1* genomic clone. Ten-day-old conidia of *N. crassa* wild-type strain 73a (Table 1) were electroporated with 1 μg of pSVK7 linearized with SphI, as described previously (37, 69), and transformants were selected on sorbose medium (13) containing hygromycin B. Genomic DNA was extracted from transformants by using the Puregene kit according to the manufacturer's protocol (Gentra Systems, Minneapolis, Minn.). To identify homologous and ectopic integrations, genomic DNA from transformants was subjected to Southern analysis after digestion with NcoI (37). The 1.8-kb 5′ DNA flank (SalI-EcoRV) from pSVK3 was used as a probe. Heterokaryotic gene replacement strains without ectopic integrations were crossed to the wild-type strain 74A (Table 1). The progeny were selected on sorbose medium with hygromycin B. Purity of strains was verified by Southern analysis as described above.

To complement the *gng-1* mutation in *trans*, the *gng-1* genomic clone was inserted into the *his*-3 targeting vector pRAUW122 (2). Homologous recombination of the pRAUW122 vector into the *his-3* locus of a *his-3* auxotrophic mutant (Fungal Genetics Stock Center [FGSC] #6103) leads to reconstitution of histidine prototrophy; any DNA inserted next to the *his-3* gene in pRAUW122 is also efficiently integrated at the *his-3* locus. The rescue plasmid pSVK17 was constructed as follows: genomic clone #2213 was linearized with BamHI, ends were filled using DNA polymerase I (Klenow), and the plasmid was subsequently

TABLE 2. Oligonucleotides used in this study

Name	Sequence
5GNG1	5′-CGGAATTCCATTGTCGCCCACGTC-3′
3GNG1	5′-CGGGATCCACCGGCCCCCAAACAC-3′
LEXA-GNB1-BAMH-FW	5′-GGGATCCGTATGGACTCCCGATCAA-3′
LEXA-GNB1-PST-RVB	5′-GGCTGCAGAAAGTGACGCGTCGTGA-3′
GNA-2-ECORI-FW	5′-CGGAATTCGAGTGGAAAAGGGACC-3′
GNA-2-BAMH1-RV	5′-GGTGGATCCAAAATGACAAAGGGC-3′
GNA3THA-FW	5′-GTGATGAATTCGGGCGCATGCATG-3′
GNA3THA-RV	5′-GGGGTCGACATCATAGAATACCGG-3′
GNG1-FLAG-XBA-FW	5′-GGTCTAGAATGGATTACAAGGATGACGACGATAAGATGCCTCAGTACGCCTCTCGCG-3′
GNG1-FLAG-ECOR-RV	5′-CCGAATTCAATTTACATGACGACGCAGCACCCGCT-3′

digested with XbaI. The resulting 6.5-kb fragment was then inserted into pRAUW122. To construct a recipient for *his-3* targeting, a Δ*gng-1 matA* strain (5-12) was crossed to a *his-3 mata* strain (his3a) and Δ*gng-1 his-3* progeny were selected (see Table 1). A Δ*gng-1 his-3* strain (113-1) was transformed by electroporation with pSVK17, and transformants were plated on histidine-free sorbose medium supplemented with hygromycin B. Heterokaryons containing the wild-type *gng-1* allele integrated at the *his-3* locus were identified by Southern analysis using the 1.8-kb 5′ DNA flank fragment (excised using SalI-EcoRV) from pSVK3 as a probe (data not shown). Genomic DNA was digested with ApaI. Heterokaryons with homologous recombination at the *his-3* locus were isolated after microconidiation (21) to obtain Δ*gng-1*::*hph*$^+$ *gng-1*$^+$::*his-3*$^+$ strains.

Isolation of Δ*gnb-1* Δ*gng-1* double mutants. Based on phenotypic analysis, both Δ*gnb-1* and Δ*gng-1* mutants are female sterile (see Fig. 3). To isolate Δ*gnb-1* Δ*gng-1* double mutants, a forced heterokaryon was made between Δ*gnb-1 his-3 mata* and the helper strain *a*^{m1} *ad-3B cyh-1* (FGSC 4654), and it was used as a Δ*gnb-1* female in crosses (29) (Table 1). Conidia from a Δ*gng-1* strain of opposite mating type (*matA*) were used as the male. The presence of the Δ*gng-1* and Δ*gnb-1* mutations in progeny was verified by Southern analysis as described above (for *gng-1)* or as described previously (for *gnb-1* [80]).

Northern and Western analyses. The tissue samples for Western and Northern analyses were obtained as follows. For submerged cultures, 500 ml of liquid VM was inoculated with conidia at a final concentration of 10^6 cells/ml. Cultures were incubated in the dark at 30°C with shaking at 200 rpm for 8 or 16 h, as indicated. Differentiated tissues were grown on solid medium (VM or SCM) overlaid with cellophane (Bio-Rad, Hercules, Calif.). VM plates were incubated in the dark at 30°C for 3 days. SCM plates were grown in constant light at 25°C for 6 days. For perithecial tissues, 6-day-old cultures grown on SCM were fertilized with the wild-type strain of opposite mating type and incubated for an additional 3 days under the same conditions as those used for unfertilized SCM plates.

For Northern analysis, total RNA was extracted from tissue ground in liquid nitrogen using a previously described protocol (5). Samples containing 20 μg of total RNA were subjected to Northern analysis as described elsewhere (57). Probe templates were generated as follows. For *gng-1*, a 279-bp PCR product was amplified from the *gng-1* cDNA clone pSVK1 by ExTaq (Takara, New York, N.Y.) using the 5GNG1 and 3GNG1 primers (Table 2). pSVK1 contains the entire *gng-1* ORF (without introns) cloned in pET11a (Invitrogen, Carlsbad, Calif.). For *gnb-1*, a 1,074-bp PCR product was amplified from cDNA clone pBR2 using primers LEXA-GNB1-BAMH-FW and LEXA-GNB1-PST-RV (Table 2). Plasmid pBR2 corresponds to the entire ORF (no introns) of *gnb-1* amplified by reverse transcriptase PCR (Access RT-PCR; Promega) and subsequently cloned into the pGEM-T vector (Promega). A 5.6-kb EcoRI-ClaI fragment from pPNO5 (37) was the source of *gna-1*, while a 967-bp PCR product corresponding to *gna-2* was amplified from cDNA clone 13M2A5-2 (68) using GNA-2-ECORI-FW and GNA-2-BAMHI-RV as oligomers (Table 2). A template for *gna-3* was generated by amplification of a 1,068-bp PCR product from pAK1 (41) using GNA3THAFW and GNA3THARV as primers (Table 2). All probe templates were labeled using the random primer method according to the manufacturer's protocol (Promega).

For Western analysis, plasma membrane fractions were isolated as described previously (10, 68) and protein concentration was determined using the Bradford protein assay (Bio-Rad). Samples containing 30 μg of total protein were denatured and solubilized in sodium dodecyl sulfate-polyacrylamide gel electrophoresis (SDS-PAGE) sample buffer (62.5 mM Tris-HCl [pH 6.8], 10% glycerol, 2% SDS, 1% β-mercaptoethanol, 0.005% bromphenol blue) by boiling for 5 min. To detect GNA-1, GNA-2, GNA-3, and GNB-1, protein samples were resolved using SDS–10% PAGE and transferred to a polyvinylidene difluoride (PVDF) membrane (37, 68). The primary polyclonal rabbit antibodies against GNA-1, GNA-2, GNA-3, and GNB-1 were used at dilutions of 1:3,000, 1:5,000, 1:1,000, and 1:5,000, respectively (3, 37, 38, 43, 80). A horseradish peroxidase conjugate (Bio-Rad) was used as the secondary antibody at a dilution of 1:10,000. Detection was performed using a Biochemi system (UVP, Upland, Calif.) with chemiluminescence detection reagents used according to the manufacturer's protocol (Pierce, Rockford, Ill.).

To produce a specific antiserum for GNG-1, the amino acid sequence corresponding to the extreme amino terminus (plus a cysteine for coupling to the resin: CQYASRDVGDPSQIKKN) was synthesized (United States Biological, Swampscott, Mass.) and used as an antigen to produce a rabbit polyclonal antibody (Cocalico Biologicals, Reamstown, Pa.). The plasma membrane fraction was isolated from strains as described above. Samples containing 30 μg of total protein were separated on a SDS–15% PAGE gel and transferred to a PVDF membrane (Millipore Corp., Bedford, Mass.). The primary antibody was used at a dilution of 1:3,000. The secondary antibody treatment and chemiluminescence system were the same as those described above.

Coimmunoprecipitation studies. A construct containing the *gng-1* ORF with the FLAG epitope tag at the amino terminus was targeted to the *his-3* locus in a Δ*gng-1 his-3* strain to facilitate coimmunoprecipitation experiments. To generate a FLAG fusion construct, the GNG1-FLAG-XBA-FW primer was engineered to contain a 24-bp sequence encoding the FLAG epitope (DYKDDDDK) (7). The *gng-1* ORF was amplified by PCR (LA Taq; Takara) from pSVK1 using GNG1-FLAG-XBA-FW and GNG1-FLAG-ECOR-RV as oligomers (Table 2) with designed XbaI (5′ end) and EcoRI (3′ end) restriction sites. The resulting 323-bp PCR product was cloned into pGEM-T (Promega, Madison, Wis.), yielding pBR5. A 319-bp insert containing the FLAG-*gng-1* fusion construct was subsequently released from pBR5 with XbaI and EcoRI and was cloned in the *his-3*-targeting vector pMF272 (26), generating pBR6. pMF272 was originally constructed for overexpression of green fluorescent protein (GFP) fusion proteins under control of the *N. crassa ccg-1* promoter (26). In pBR6, the GFP gene has been replaced with the XbaI-EcoRI fragment from pBR5. Ten-day-old conidia from Δ*gng-1 his-3* strain #113 were transformed with pBR6, and transformants were plated on FIGS plates. Strains with homologous recombination events were identified by Southern analysis using the 8.8-kb HindIII fragment from pRAUW122 as a probe, and homokaryons were purified using the microconidiation technique (21).

For coimmunoprecipitation experiments, conidia were inoculated in 500 ml of liquid VM at a final concentration of 10^6 cells/ml. Cultures were incubated in the dark at 30°C with shaking at 200 rpm for 16 h, harvested by filtration, and ground in liquid nitrogen. The plasma membrane fraction was isolated, and protein concentrations were determined as described above. To solubilize membrane-associated proteins, samples containing 2 mg of total protein were adjusted to 360 μl with the extraction buffer (see above). Subsequently, 40 μl of 5% Triton X-100 was added, and the solution was incubated on ice for 15 min. The mixtures were then centrifuged (21,000 × *g* for 15 min at 4°C) to remove insoluble material. The supernatant was diluted with an equal volume of 2× coimmunoprecipitation buffer (20 mM Tris-Cl [pH 7.5], 300 mM NaCl), and 80 μl of anti-FLAG M2-agarose slurry (Sigma, St. Louis, Mo.) was added. The suspension was incubated at 4°C on a rotating shaker for 3 h. Afterwards, the agarose beads were collected by centrifugation (1,000 × *g* for 1 min at 4°C) and washed twice with ice-cold 1× Tris-buffered saline. An aliquot (50 μl) of 2× sample buffer (25 mM Tris-HCl [pH 6.8], 4% SDS, 20% [vol/vol] glycerol, 0.004% bromphenol blue) was added to the agarose beads, and the mixture was incubated at 95°C for 3 min. The samples were then centrifuged (21,000 × *g* for 30 s at room temperature). Aliquots of supernatant (40 μl) were then resolved using a 10 (GNB-1 detection) or 15% (GNG-1 detection) SDS-PAGE gel, and the

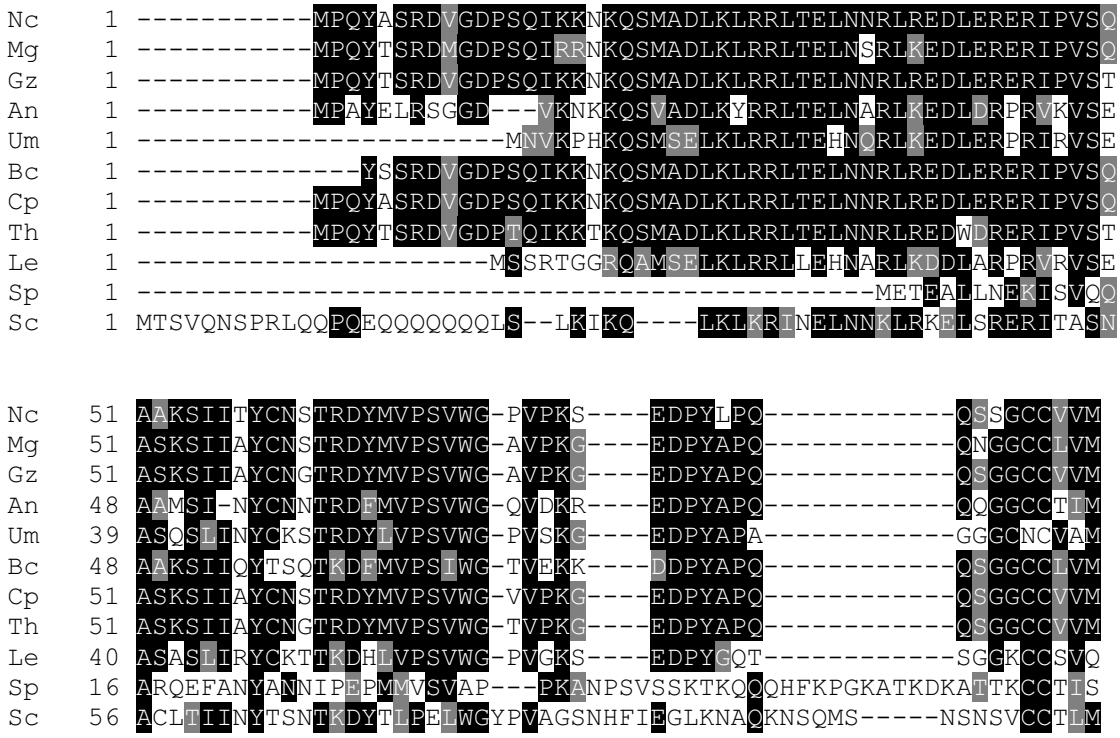

FIG. 1. Alignment of GNG-1 with other fungal Gγ protein sequences. ClustalW (http://www.embl.co.uk) was used to align Gγ protein sequences from *N. crassa* (Nc; GNG-1; NCU00042.1) with Gγ subunits from *M. grisea* (Mg; MG10193.4), *G. zeae* (Gz; accession no. 387411.1), *A. nidulans* (An; accession no. XT 4068791.1), *U. maydis* (Um; UM 06109.1), *Botrytis cinerea* (Bc; accession no. AL 114303), *C. parasitica* (Cp; accession no. CB 688576), *T. harzianum* (Th; accession no. CF875833), *L. edodes* Gg1 (Le; accession no. AAP 13581.1), *S. pombe* Git11 (Sp; accession no. NP 596681), and *S. cerevisiae* Ste18p (Sc; accession no. CAA 89613). BOXSHADE (www.ch.embnet.org) was used to indicate identical (black shading) and similar (gray shading) amino acid residues.

proteins were subsequently transferred to PVDF membranes (Millipore Corp.). Western analysis was performed as described above, using anti-FLAG M2 monoclonal (1:1,000; Sigma), anti-GNG-1 (1:3,000), and anti-GNB-1 (1:5,000) as primary antibodies.

Phenotypic analysis. To determine apical extension rates, 1 μl of a conidial suspension was inoculated in the center of VM plates and the plates were incubated at 30°C in the dark. The colony diameter was measured at 2-h intervals. To analyze phenotypes in submerged cultures, liquid VM was inoculated with conidia at a final concentration 10^6 cells/ml and incubated with shaking at 200 rpm for 16 h at 30°C. Cultures were then viewed and photographed using a BX41 fluorescent microscope and a C-4040 digital camera (Olympus, Lake Success, N.Y.). Unfertilized (6-day-old protoperithecia) and fertilized (3-day-old perithecia) female tissues were grown on SCM plates in light and were observed using an SZX9 stereomicroscope with an ACH 1× objective lens outfitted with the C-4040 digital camera (Olympus).

For trichogyne pheromone attraction assays (7, 8, 44), cultures were grown for 6 days on 2% water agar. Chemoattraction between trichogynes and microconidia was observed using a BX41 fluorescent microscope with UM Plan Fluorite objective lenses (Olympus) as described above.

Measurement of intracellular steady-state cAMP levels. For measuring in vivo cAMP levels, 16-h submerged cultures and tissues grown on VM plates for 3 days at 30°C in the dark and SCM plates incubated at 25°C in constant light were ground in liquid nitrogen and extracted as previously described (38). cAMP levels were quantified using a protein binding assay following the manufacturer's instructions (Amersham Pharmacia Biotech, Piscataway, N.J.). The protein concentration was determined using the bichinonic acid method (Pierce) as described elsewhere (38).

Nucleotide sequence accession number. The GenBank accession number for the *gng-1* cDNA clone a8h02ne is AY823297.

RESULTS

***gng-1* isolation, gene structure analysis, and mRNA expression profile.** Two cDNA clones (b7a10ne and a8h02ne) similar to the *S. cerevisiae* Gγ subunit Ste18p were identified using BLAST (1) in the *Neurospora* database at the University of Oklahoma (http://www.genome.ou.edu). The *gng-1* ORF is 279 bp, and the predicted GNG-1 protein consists of 93 amino acid residues with a molecular mass of 10 kDa (Fig. 1). GNG-1 shows relatively high identity to Gγ proteins from other filamentous fungi: 90% to *G. zeae*, 92% to *C. parasitica*, 86% to *Trichoderma harzianum*, 86% to *M. grisea*, 65% to *A. nidulans*, and 55% to *Ustilago maydis*. Interestingly, *N. crassa* GNG-1 shares only 40% identity with *S. cerevisiae* Ste18p (76) and even less identity with *S. pombe* Git11 (9%) (45), indicating evolutionary divergence between filamentous fungi and yeasts. In addition, as a group, fungal Gγ proteins display very little identity (less than 20%) to mammalian Gγ proteins (data not shown). Predicted Gγ proteins from *U. maydis* (UM 06109.1) and *M. grisea* (MG10193.4) were identified in genome databases at http://www.broad.mit.edu/annotation/fungi. However, the positions of introns and exons in the two genes were predicted incorrectly by the automatic gene caller. Therefore, both genes were annotated manually, and the resulting protein sequences were used in the alignment (Fig. 1).

In order to isolate a genomic clone, the 1.2-kb insert of cDNA clone a8h02ne was used to screen a BARGEM-7λ genomic library (53). The screen resulted in isolation of two genomic clones designated #31 (4.5-kb insert) and #2231 (6.5-kb insert). The entire nucleotide sequence of the a8h02ne cDNA and partial nucleotide sequence of genomic clone #31

were used to determine the gene structure of *gng-1* (Fig. 2A). The *gng-1* gene contains one 96-bp intron in the ORF, from +162 to +257. Another 315-bp intron is present in the 5′-untranslated region (UTR) of the mRNA (−510 to −196). All of the exon-intron boundaries conform to the GT-AG rule for intron splice sites.

The sequence of the 5′ region upstream of the *gng-1* ORF was obtained (http://www.broad.mit.edu/annotation/fungi/neurospora) and analyzed for potential transcriptional regulatory motifs (Fig. 2A). No identifiable pyrimidine-rich regions (31) or TATA box consensus sequences (75) were present. Nevertheless, two putative transcriptional regulatory motifs were observed: one CTTTG at −320 (4) and one CCAAT box at −453 (31).

In order to elucidate the expression of *gng-1* throughout development, Northern analysis was used to examine *gng-1* transcript levels in conidia, 8- and 16-h submerged cultures, and VM and SCM plates. *gnb-1* message levels were also measured during the experiment. A 1.2-kb *gng-1* transcript was detected in all tissues (Fig. 2B and data not shown). This size is similar to the insert sizes (1,198 bp) of the two independent cDNA clones (b7a10ne and a8h02ne). The results show that *gng-1* is differentially expressed during the life cycle of *N. crassa* and that the highest expression levels of *gng-1* are in 8-h submerged cultures and protoperithecial tissue from SCM plates (Fig. 2B). The lowest levels of *gng-1* were detected in conidia and in tissues grown on VM plates. Comparison of *gnb-1* and *gng-1* message levels shows that these two genes share a similar expression pattern (Fig. 2B) (80). A possible exception is on SCM plates, where *gng-1* may have higher relative expression levels than *gnb-1*. Observation of similar expression profiles has also been reported for the single Gβ and Gγ in *Dictyostelium discoideum* (83).

Deletion of *gng-1* by targeted gene replacement and isolation of a Δ*gng-1 gng-1*$^+$-complemented strain. A Δ*gng-1* mutant was isolated after electroporation of a wild-type strain with a construct in which the *gng-1* ORF was replaced by the hygromycin B cassette (Fig. 2A) (66). Genomic DNA from transformants was digested with NcoI and subjected to Southern analysis using the 1.8-kb DNA fragment (SalI-EcoRV) from pSVK3 as a probe (Fig. 2C). Under these conditions, the wild-type strain produces a 5.7-kb hybridizing fragment, while a 2.8-kb fragment is detected in Δ*gng-1* nuclei (Fig. 2C). Transformants exhibiting homologous recombination at the *gng-1* locus were crossed to a wild-type strain of opposite mating type to produce homokaryotic Δ*gng-1* mutant progeny. The genotype of homokaryons was verified by Southern analysis (data not shown). Δ*gng-1* Δ*gnb-1* double mutants were constructed by crossing the Δ*gnb-1* as a female, with sheltering in a heterokaryon (see Materials and Methods). Northern analysis showed that Δ*gng-1* and Δ*gnb-1* Δ*gng-1* strains lack *gng-1* mRNA (Fig. 2D). Western analysis using a rabbit polyclonal antibody raised against a GNG-1 peptide sequence (see Materials and Methods) demonstrated that Δ*gng*-1 and Δ*gnb-1* Δ*gng-1* mutants do not produce the corresponding GNG-1 protein (Fig. 2E).

The Δ*gng-1* mutation was complemented in *trans* using the 6.5-kb *gng-1* genomic fragment in the *his-3* targeting vector pRAUW123 (2). Transformants were screened for conferral of histidine prototrophy. Homokaryons were obtained by using microconidial isolation (21). Both *gng-1* mRNA and GNG-1 protein were detected at appreciable levels in Δ*gng-1 gng-1*$^+$-complemented strains (Fig. 2D and E).

Δ*gng-1* strains are female sterile and male fertile. In *N. crassa*, sexual development is induced by nitrogen starvation, with formation of female reproductive structures (protoperithecia) containing specialized hyphae, termed trichogynes (55). Trichogynes exhibit chemotropic growth towards male gametes (conidia or other vegetative cells) of opposite mating type (9), followed by fusion and recruitment of a male nucleus to the base of the protoperithecium. The nuclei from the male and female parents recognize one another and migrate to croziers (ascogenous hyphae), where they undergo mitosis. Subsequent fusion of male and female nuclei is followed by two meiotic divisions and one episode of postmeiotic mitosis. Each resulting ascus contains eight homokaryotic, haploid ascospores. About 200 to 400 asci are enclosed in each mature fruiting body (perithecium).

Previous studies have shown that Δ*gnb-1* mutants are female sterile but are fertile as males during sexual crosses (80). Δ*gnb-1* mutants are able to form protoperithecia but fail to develop fruiting bodies after fertilization (80) (Fig. 3A). Δ*gng-1* strains and Δ*gng-1* Δ*gnb-1* double mutants exhibit a phenotypic pattern identical to that of Δ*gnb-1* strains (Fig. 3A). Although they produce reproductive structures, development of normal perithecia after fertilization is blocked (Fig. 3A), and no ascospores are produced (data not shown). In contrast, Δ*gng-1 gng-1*$^+$-rescued strains are phenotypically identical to the wild type (Fig. 3A).

Our laboratory has demonstrated that Δ*gnb-1* mutants are deficient in both trichogyne attraction and perithecial development (44, 80). In order to determine whether a similar defect is present in Δ*gng-1* strains or Δ*gng-1* Δ*gnb-1* double mutants, microconidia of opposite mating type were applied at a distance from wild-type, Δ*gng-1*, Δ*gnb-1*, or Δ*gng-1* Δ*gnb-1* double mutant protoperithecia. Growth of trichogyne tips towards male cells was then followed microscopically (8, 44). In a previous study (44), Δ*gna-1* and Δ*gnb-1* mutants did not display directional migration but instead grew in random directions and failed to undergo fusion with male cells, even when in direct contact. Similarly, trichogynes of Δ*gng-1* and Δ*gnb-1* Δ*gng-1* strains did not respond to microconidia and exhibited random orientation on the agar surface during this analysis (Fig. 3B). Δ*gng-1 gng-1*$^+$-complemented strains resembled the wild type, with normal trichogyne migration and fusion with microconidia (Fig. 3B). These data support the hypothesis that GNA-1 and Gβγ (GNB-1/GNG-1) are essential for trichogyne chemotropism during the pheromone response and for subsequent fusion with male gametes. The observations from previous work suggested that GNA-1 is coupled to PRE-1 (the *matA* pheromone receptor), because Δ*pre-1* strains exhibit the same defects in trichogyne chemoattraction as Δ*gna-1* mutants (44).

Δ*gng-1* mutants conidiate inappropriately in submerged culture. During vegetative growth, *N. crassa* produces tubular filaments (hyphae) characterized by tip-based polarized growth. We analyzed the rate at which strains extended vegetative hyphae on VM medium. Apical extension rates of Δ*gnb-1* and Δ*gng-1* single and double mutants are similar to those of the wild type and Δ*gna-3* mutants (41, 80, and data not

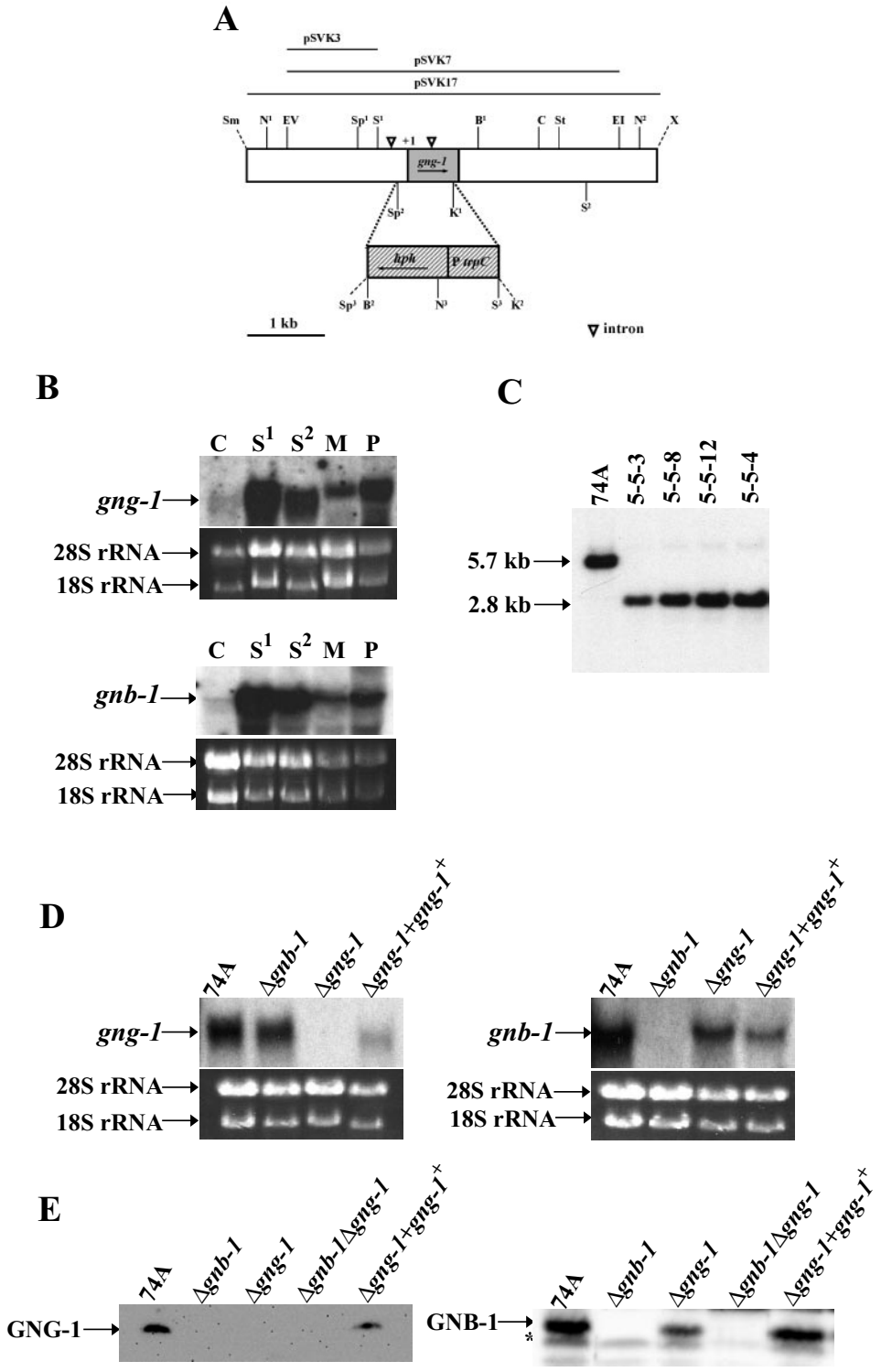

FIG. 2. Structure of the *N. crassa gng-1* genomic region and construction of Δ*gng-1*- and Δ*gng-1 gng-1*$^{+}$-rescued strains. (A) *gng-1* genomic clone and gene replacement vector. The grey area indicates the *gng-1* ORF, and the hatched region corresponds to the gene conferring hygromycin resistance, *hph*, under control of the *A. nidulans trpC* promoter. The dashed lines illustrate the region replaced by *hph* that is between the second SpeI and first KpnI sites. The open triangles indicate intron positions (−511 to −197; +162 to +258). The arrows show the direction of transcription of *gng-1* and *hph*. Abbreviations for restriction sites: N, NcoI; EV, EcoRV; Sp, SpeI; S, SalI; K, KpnI; B, BamHI; C, ClaI; St, StuI; E, EcoRI; X, XbaI; Sm, SmaI. KpnI^{2}, SpeI^{3}, and the unique XbaI and SmaI are artifacts of cloning. pSVK3 was the probe used for Southern analysis (see the legend to panel B). pSVK7 was used as the gene replacement construct, while the portion of *gng-1* in pSVK17 was present in the *his-3*-targeted rescue construct. (B) Expression of *gng-1* and *gnb-1* during the *N. crassa* life cycle. Samples from wild-type strain 74A tissues (20 μg of total RNA) were subjected to Northern analysis using as probes a 1,074-bp PCR product amplified from pBR2 for detection of the *gnb-1* transcript and a 279-bp PCR product amplified from pSVK1 to detect the *gng-1* ORF. The tissues used in the experiment were as indicated. C,

shown) but differ from those of Δ*gna-1* strains that display reduced apical extension rates (37).

Asexual spore formation (conidiation) is induced in wild-type strains of *N. crassa* cultured on solid medium. In contrast, submerged cultures form vegetative nonconidiating hyphae unless starved for carbon or nitrogen or exposed to stress conditions, such as high temperature (54, 67). Our laboratory previously showed that Δ*gna-1*, Δ*gna-3*, and Δ*gnb-1* strains conidiate inappropriately in submerged culture; in the case of Δ*gna-1* strains, submerged conidiation is cell density dependent (39, 41, 80).

The conidiation patterns of Δ*gnb-1*, Δ*gng-1*, and Δ*gnb-1* Δ*gng-1* mutants cultured on solid medium are similar (80 and data not shown), with the mutants exhibiting shorter aerial hyphae and increased conidiation relative to the wild type. Like Δ*gna-1*, Δ*gna-3*, and Δ*gnb-1* strains, Δ*gng-1* single and Δ*gnb-1* Δ*gng-1* double mutants also form conidia in 16-h submerged cultures (Fig. 4). Rescued Δ*gng-1 gng-1*$^+$ strains are phenotypically identical to the wild type (Fig. 4).

Δ*gng-1* and Δ*gnb-1* mutants have decreased levels of intracellular cAMP. Study of fungal Gα subunits has revealed functions for these proteins in regulation of cAMP levels. In *N. crassa*, GNA-1 is required for GTP-dependent adenylyl cyclase activity, while GNA-3 regulates the levels of the adenylyl cyclase protein (CR-1) (38, 41). Levels of cAMP are greatly reduced in both submerged and plate cultures of Δ*gna-3* mutants, and many defects of Δ*gna-3* strains can be reversed by supplementation with cAMP (41). On the other hand, Δ*gna-1* mutants have normal intracellular cAMP levels during submerged growth but low levels in cultures grown on solid media. The normal concentration of cAMP in submerged cultures may result from a compensatory mechanism involving reduced cAMP-phosphodiesterase activity (38). Δ*gna-2* mutants have normal cAMP amounts in submerged cultures and on VM plates but smaller amounts on SCM solid medium (38). Δ*gna-1* Δ*gna-2* strains have normal cAMP levels in submerged cultures but greatly reduced concentrations on VM and SCM plates (38). Similar to Δ*gna-1* and Δ*gna-2* strains, Δ*gnb-1* mutants have normal levels of cAMP in submerged cultures but low cAMP levels on VM (Table 3) (80) and SCM plates (Table 3). Furthermore, like Δ*gna-1* and Δ*gna-2* mutants, Δ*gnb-1* strains have normal levels of CR-1 protein but reduced GTP-dependent adenylyl cyclase activity (80).

The results from previous studies indicating effects on cAMP levels due to loss of heterotrimeric G proteins in *N. crassa* prompted measurement of cAMP levels in Δ*gng-1* strains. As expected, Δ*gng-1* strains have concentrations of cAMP very similar to those of Δ*gnb-1* mutants (Table 3). Wild-type amounts of cAMP are produced in submerged cultures, while reduced levels are obtained when Δ*gng-1* mutants are cultured on VM (55% of wild type) or SCM (21% of wild type) plates.

Δ*gng-1* strains have reduced Gβ and Gα protein levels. Gβ and Gγ subunits form a tight complex and are not known to dissociate from one another in vivo. Coexpression of the Gβ and Gγ subunit and the presence of an intact CaaX domain in the Gγ protein are required for plasma membrane targeting (58, 60). Mutation of Gγ genes has been shown to suppress the level of Gβ protein(s) in various organisms (34, 62, 71). To determine whether a similar mechanism exists in *N. crassa*, the plasma membrane fraction of Δ*gng-1* and Δ*gnb-1* mutants was subjected to Western analysis using GNG-1- and GNB-1-specific antisera (Fig. 2E). The results demonstrate that the amount of GNB-1 was reduced ~60% in Δ*gng-1* mutants (Fig. 2E) and that GNG-1 is almost completely absent from the plasma membrane of Δ*gnb-1* mutants (Fig. 2E). We were not able to detect GNG-1 in nonmembrane fractions of wild-type or mutant strains (data not shown), presumably due to low concentrations of GNG-1 in the cytosol. Interestingly, the levels of GNB-1 protein in cytosolic fractions from the Δ*gng-1* mutant and wild-type are comparable (data not shown), demonstrating that the major reduction in GNB-1 levels occurs in plasma membrane fractions of the Δ*gng-1* strain. The effect of the mutations appears to be largely posttranscriptional, as either normal (*gng-1* in Δ*gnb-1*) or 50% reduced (*gnb-1* in Δ*gng-1*) levels of the corresponding mRNAs are present in those cases where the partner protein is absent (Fig. 2D). In addition, the reduced amount of *gnb-1* in Δ*gng-1* mutants is similar to that of rescued Δ*gng-1 gng-1*$^+$ strains that have normal levels of GNB-1 (Fig. 2E) and are phenotypically comparable to the wild type.

Tethering of the Gβ protein by isoprenylated Gγ also facilitates interactions between Gβ and its other partner protein, Gα, at the plasma membrane. Deletion of the Gγ subunit can not only affect the levels of Gβ but also affect the levels of Gα proteins. For example, it has been shown in mice that $G\gamma_7$ is required for the stability of a G-protein heterotrimer ($\alpha_{olf}\beta\gamma_7$), in that loss of $G\gamma_7$ results in an 82% reduction in $G\alpha_{olf}$ protein levels in *Gng7*$^{-/-}$ mutant mice (61). Deletion of the mouse $G\gamma_3$ gene, which results in a phenotype distinct from that of *Gng7*$^{-/-}$ mice, leads to reduced levels of $G\beta_2$ and $G\alpha_{i3}$ proteins. And, as mentioned above, deletion of the Gβ gene *gnb-1* suppresses the level of Gα subunits in *N. crassa* (80).

Because GNG-1 is the only Gγ subunit in *N. crassa* and, by extension, is the only Gγ subunit capable of interacting with GNB-1, it was reasonable to test whether loss of *gng-1* would affect expression of the three Gα proteins. Western analysis was used to measure levels of Gα proteins in wild-type, Δ*gnb-1*, Δ*gng-1*, and Δ*gnb-1* Δ*gng-1* strains in three different tissues:

conidia; S^1, 8-h submerged cultures; S^2, 16-h submerged cultures; M, cultures grown for 3 days at 30°C on solid VM in the dark; P, cultures grown for 6 days at 25°C on SCM under light. Amounts of the major RNA species are shown as loading controls. (C) Southern analysis. Genomic DNA was digested with NcoI, and the 1.8-kb SalI-EcoRV fragment from pSVK3 was used as a probe. Strains 5-5-3, 5-5-8, and 5-5-12 are purified homokaryotic Δ*gng-1* mutants. Strain 5-4 is a Δ*gnb-1* Δ*gng-1* double mutant. (D) Northern analysis of mutant and wild-type strains. Samples containing 20 μg of total RNA isolated from 16-h submerged cultures were subjected to Northern analysis using a 1,074-bp PCR product amplified from pBR2 to detect the *gnb-1* transcript and a 279-bp PCR product amplified from pSVK1 to detect *gng-1* mRNA. The strains used in the analysis are 74A (wild type), Δ*gng-1* (5-5-12), Δ*gnb-1* (42-8-3), and Δ*gng-1* + *gng-1*$^+$ 113-1. rRNA loading controls are as in panel B. (E) GNG-1 and GNB-1 protein levels in the wild type and mutants. Samples containing 30 μg of protein from plasma membrane fractions of 16-h submerged cultures were subjected to Western analysis using the GNG-1 and GNB-1 antibodies. The strains used in the analysis were 74A (wild type), Δ*gng-1* (5-5-12), Δ*gnb-1* (42-8-3), Δ*gnb-1* Δ*gng-1* 5-4, and Δ*gng-1* + *gng-1*$^+$ 113-1. The asterisk indicates a nonspecific band in the GNB-1 Western blot.

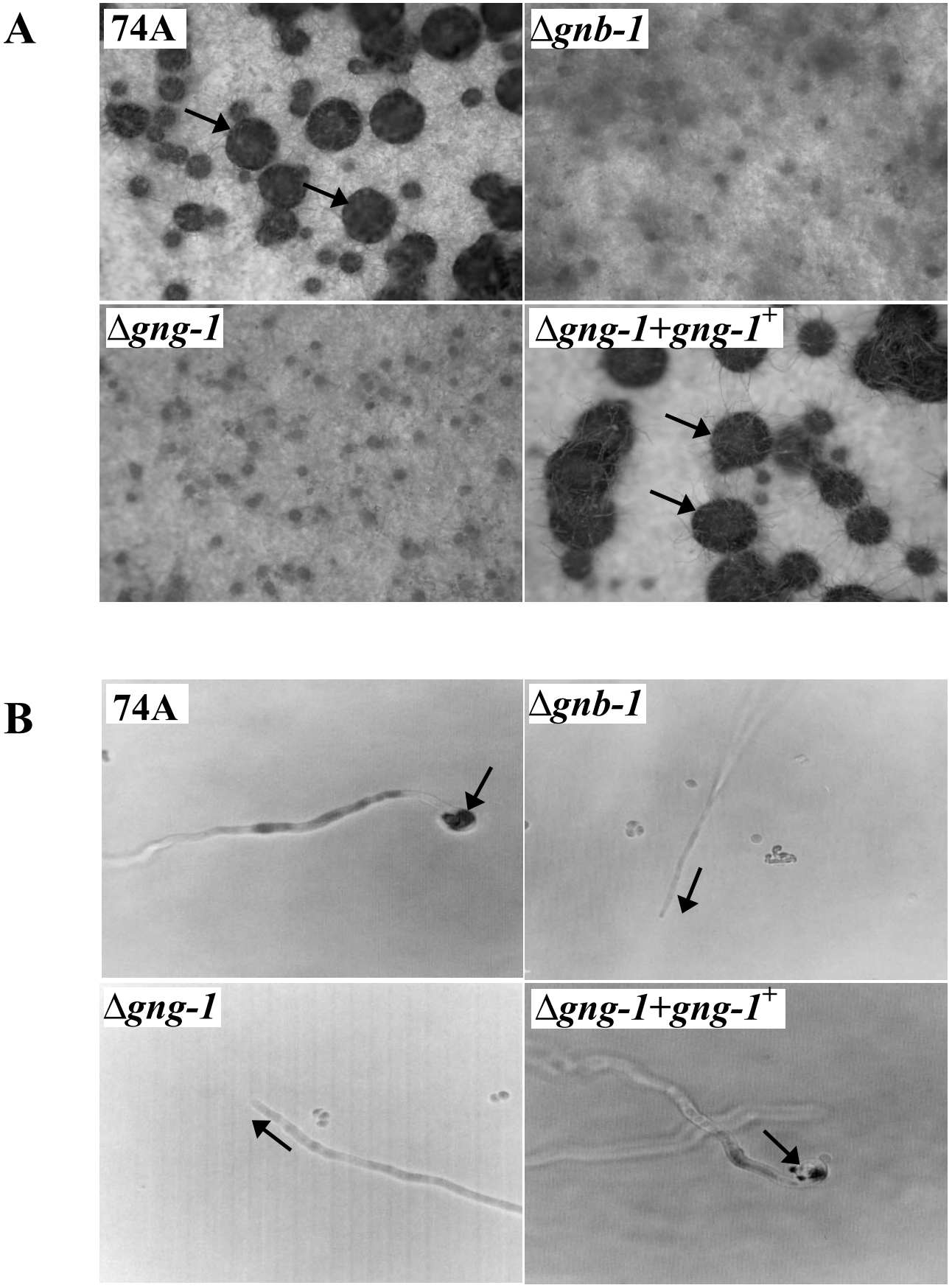

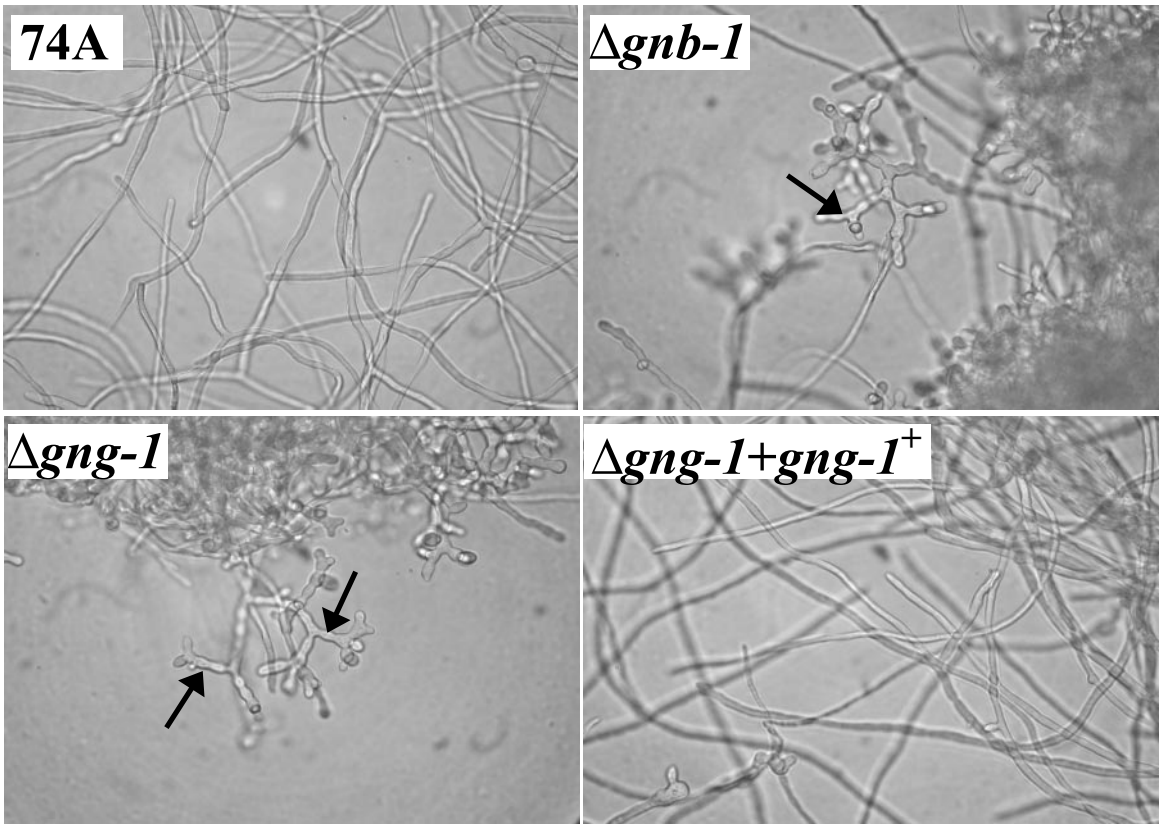

FIG. 4. Phenotypes in submerged culture. Cultures grown for 16 h at 30°C under submerged conditions with shaking were photographed at ×400 magnification. Arrows indicate conidiophores formed in Δ*gng-1* and Δ*gnb-1* cultures.

16-h submerged cultures and VM and SCM plate cultures (Fig. 5A, B, and C). The amounts of GNA-1, GNA-2, and GNA-3 were significantly diminished in all mutants analyzed, and the magnitude of the reduction was almost identical. There were significant differences observed in the levels of single Gα proteins in 16-h submerged cultures. GNA-1 and GNA-2 levels were greatly reduced in all mutants, while changes in GNA-3 were much more subtle (~30 to 50%). The amount of all Gα proteins was dramatically lowered in VM and SCM plate cultures. To determine whether the effects on Gα protein levels were pre- or posttranscriptional, we examined levels of mRNA for the *gna-1*, *gna-2*, and *gna-3* genes in 16-h submerged cultures of Δ*gng-1* and Δ*gnb-1* mutants (Fig. 5D). Similar to previous results from our laboratory (80), Gα message amounts were either normal (*gna-1* and *gna-3*) or reduced only ~50% (*gna-2*), consistent with mainly posttranscriptional regulation of Gα subunit levels in both Δ*gng-1* and Δ*gnb-1* mutants.

GNB-1 associates with GNG-1. We confirmed by coimmunoprecipitation that the GNB-1 and GNG-1 proteins physically interact in *N. crassa*. The FLAG epitope sequence was engineered at the amino terminus of the GNG-1 ORF, and the fragment was cloned into the *his-3* targeting vector, pMF272 (see Materials and Methods). The resulting plasmid was electroporated into Δ*gng-1 his-3* recipient strain #113, and *his-3*$^+$ transformants were selected on minimal medium. Homologous recombination at the *his-3* locus was verified by Southern analysis (see Materials and Methods); strains with such events were purified, and one of the strains (#5A) was used for coimmunoprecipitation studies. Phenotypic analysis of strain 5A showed that the FLAG-GNG-1 construct complemented some, but not all, of the Δ*gng-1* defects (data not shown). Although strain 5A conidiates abundantly during incubation on VM plates, conidiation is partially suppressed in 16-h submerged cultures; hyphal tips of strain 5A are swollen, but mature conidiophores similar to those of Δ*gng-1* or Δ*gnb-1* mutants were not observed. Strain 5A is also female fertile, producing perithecia and ascospores after fertilization.

Plasma membrane fractions were extracted from wild-type

FIG. 3. Phenotypic characterization during the sexual cycle. (A) Fertilized structure (perithecium) formation. Strains were cultured on solid SCM medium at 25°C for 6 days in light prior to fertilization with wild-type conidia of opposite mating type (74a or 74A). Arrows indicate perithecia (enlarged dark bodies) formed after fertilization. Photographs were taken at ×25 magnification. (B) Trichogyne attraction. Microconidia from strain 74a or 74A were used as male cells to attract trichogynes of strains (genotypes indicated on the figure) of opposite mating type. Growth and orientation of trichogynes were monitored microscopically, and photographs were taken at ×500 magnification. Arrows indicate the direction of trichogyne growth or coiling events.

TABLE 3. Intracellular cAMP levels

Strain	cAMP (pmol/mg protein)[a] (% of wild type) on:		
	Submerged culture	VM plates	SCM plates
74A (wild type)	4.49 ± 0.72 (100)	3.57 ± 0.57 (100)	6.16 ± 0.82 (100)
48-3-8 (Δ*gnb-1*)	4.21 ± 0.27 (94)	1.90 ± 0.33 (53)	1.10 ± 0.30 (18)
5-5-12 (Δ*gng-1*)	5.39 ± 0.45 (120)	1.96 ± 0.38 (55)	1.48 ± 0.52 (21)

[a] Values are the means ± the standard errors of the means, calculated using data from two independent experiments, comprising four total replicates.

(#74A), #5A (Δ*gng-1 his-3*::FLAG-GNG-1), and #113 (Δ*gng-1 his-3*) strains, and proteins were solubilized with 1% Triton X-100 (see Materials and Methods). We first analyzed the amount of tagged and untagged GNG-1 proteins present in the input membrane extracts by using Western analysis (Fig. 6A). Untagged GNG-1 and FLAG-GNG-1 were detected using two different antibodies: the GNG-1-specific peptide antibody described above and anti-FLAG antiserum. The GNG-1-specific antiserum was used to determine levels of FLAG-GNG-1 or GNG-1 protein associated with the plasma

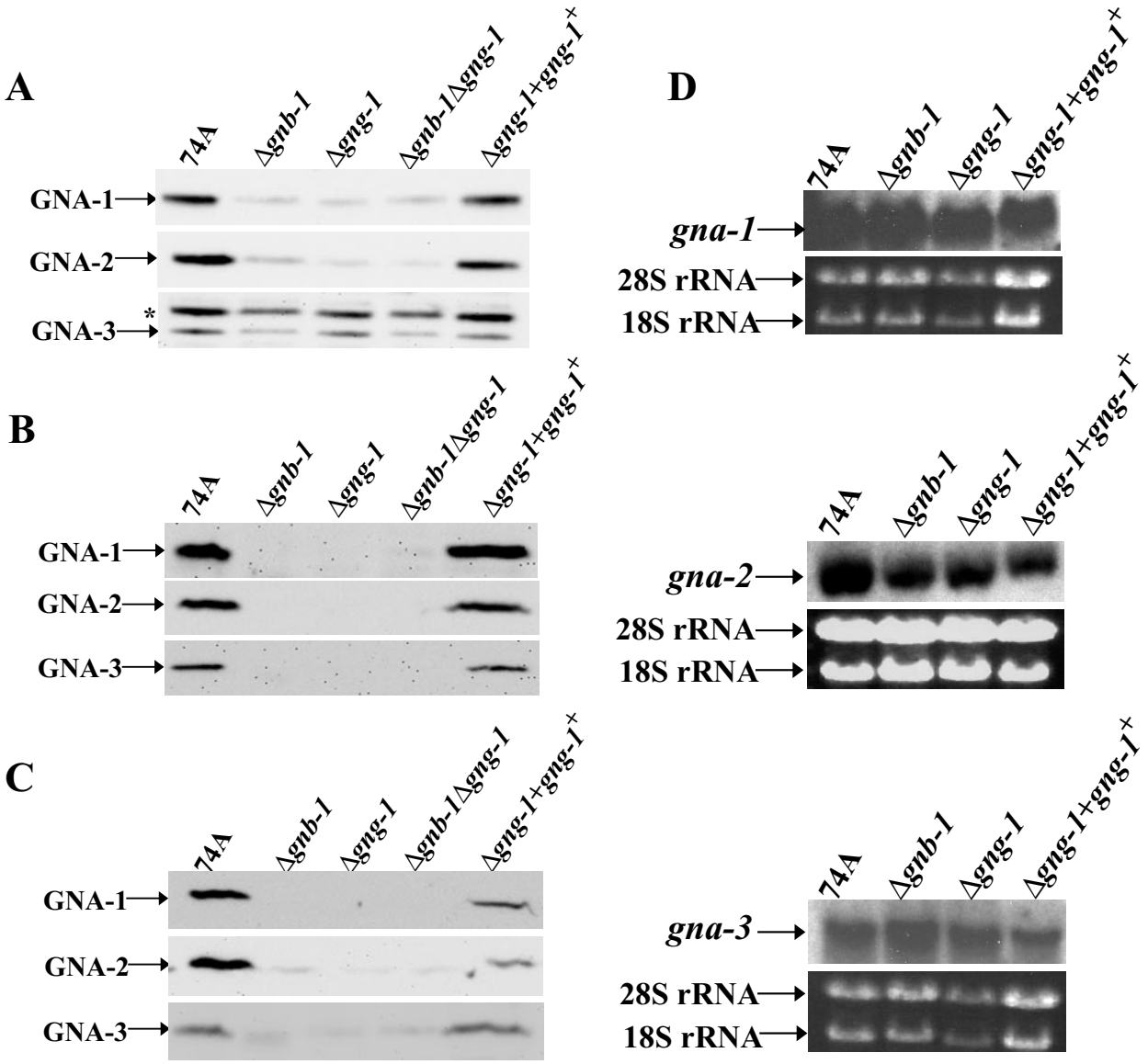

FIG. 5. Analysis of Gα protein and transcript levels. The strains used in the analysis were 74A (wild type), Δ*gng-1* (5-5-12), Δ*gnb-1* (42-8-3), Δ*gnb-1* Δ*gng-1* 5-4, and Δ*gng-1* + *gng-1*$^+$ 113-1. (A) Gα protein levels in 16-h submerged cultures. Samples containing 30 μg of protein from plasma membrane fractions were subjected to Western analysis using specific antisera (see Materials and Methods). The asterisk indicates a nonspecific band. (B) Gα protein levels in VM plate cultures. Protein samples were as indicated in panel A. (C) Gα protein levels in SCM plate cultures. Protein samples were as indicated in panel A. (D) Analysis of *gna-1*, *gna-2*, and *gna-3* transcript levels. Total RNA was extracted from 16-h submerged cultures, and 20 μg was subjected to Northern analysis using a 5.6-kb EcoRI-ClaI genomic fragment from pPNO5, a 967-bp *gna-2* PCR product amplified from plasmid 13M2A5-2, or a 1,068-bp *gna-3* PCR product amplified from pAK1 as probes. The amounts of the two major rRNA species are indicated as a loading control.

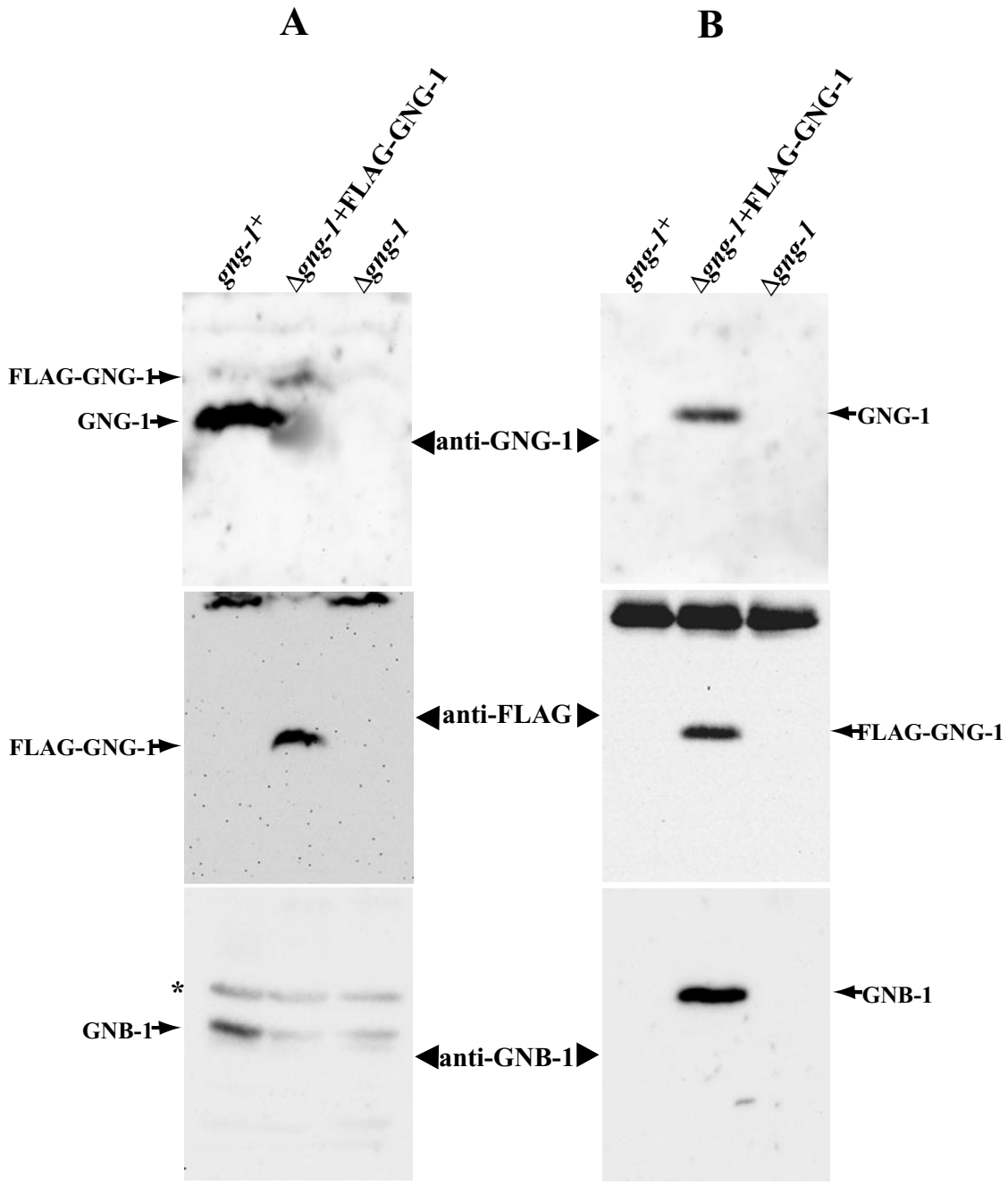

FIG. 6. Coimmunoprecipitation of GNB-1 with GNG-1. (A) Levels of GNB-1, FLAG-GNG-1, and GNG-1 proteins in plasma membrane fractions. Plasma membrane fractions were prepared from 16-h submerged cultures of *gng-1*$^+$ (74A), Δ*gng-1*$^+$ FLAG-GNG-1 (5A), and Δ*gng-1 his-3* (113) strains. Only strain 5A expresses the FLAG-GNG-1 fusion protein (see Materials and Methods). Samples containing 50 μg of total protein were resolved on 10% (GNB-1) or 15% (GNG-1 and FLAG-GNG-1) SDS-PAGE gels. GNB-1, GNG-1, and FLAG antisera were used for Western analysis (see Materials and Methods). Nonspecific bands are indicated by asterisks. (B) Immunoblot analysis after coimmunoprecipitation. The FLAG-GNG-1 protein in extracts from the indicated strains in panel A was immunoprecipitated using anti-FLAG M2-agarose (see Materials and Methods), and the precipitated proteins were examined by immunoblot analysis using anti-FLAG, anti-GNG-1, or anti-GNB-1 antibodies.

membrane (Fig. 6A, top panel). Addition of the FLAG epitope results in a protein that migrates at a larger apparent molecular weight and that can be distinguished from the untagged GNG-1 protein by using the GNG-1-specific antiserum during Western analysis (see the shift in Fig. 6A, top panel). In contrast, the FLAG antibody is specific for the tagged FLAG-GNG-1 protein present in the corresponding transformants (Fig. 6A, middle panel). The level of FLAG-GNG-1 protein in strain 5A was significantly lower than the corresponding level of untagged GNG-1 in the wild type (Fig. 6A, top panel). This

result may be explained by the difference in promoters, in that expression of the FLAG-GNG-1 construct is driven by the *ccg-1* promoter (26). The lower level of FLAG-GNG-1 versus native GNG-1 presumably leads to the observed reduction in GNB-1 amount in the FLAG-GNG-1 strain relative to that of the wild type (Fig. 6A, bottom panel) and may explain why only partial phenotypic complementation of the Δ*gng-1* mutation was observed by using the FLAG-GNG-1 construct (data not shown).

For immunoprecipitation experiments, extracts were incubated with anti-FLAG-agarose beads (see Materials and Methods), and precipitated proteins were then subjected to Western blot analysis (Fig. 6B). We were able to immunoprecipitate FLAG-GNG-1 in strain 5A by using anti-FLAG agarose beads (Fig. 6B, top and middle panels). Importantly, GNB-1 was also present in the immunoprecipitate (Fig. 6B, bottom panel). The reaction is specific for FLAG-tagged GNG-1, as no GNB-1 can be detected in precipitated material from wild-type or Δ*gng-1 his-3* recipient strains, although the former contains appreciable amounts of GNB-1 protein (Fig. 6A, bottom panel).

DISCUSSION

BLAST searches of the expressed sequence tag databases and the complete *N. crassa* genome sequence produce evidence for only one Gγ protein, GNG-1. Although we cannot rule out the possibility of another Gγ with a very different sequence, previous studies of mammals and plants have shown that Gγ proteins from the same species usually share a relatively high level of similarity (28, 49). The predicted GNG-1 protein possesses a typical Gγ secondary protein structure (2.5 helices) (63, 83) and the conserved CaaX box motif at the carboxy terminus. As shown in other species, the CaaX motif is subjected to isoprenylation (farnesylation or geranylgeranylation) at the cysteine residue, followed by proteolytic removal of the last three amino acids and methylation of the carboxy terminus (28). If the last amino acid residue (X) of the CaaX box is M, S, Q, or A, the cysteine is a substrate for farnesylation, whereas leucine (X = L) results in geranylgeranylation (59). Amino acids at the X position of the CaaX box in characterized fungal Gγ proteins are M (GNG-1 and Ste18p), S (Git11), or Q (Gg1 from *Lentinula edodes*), indicating that the CaaX motif is likely to be farnesylated.

Like Ste18p from *S. cerevisiae* and Git11 from *S. pombe*, GNG-1 contains two cysteine residues near its carboxy terminus (Fig. 1). In Ste18p, one cysteine, at position 107, is contained in the farnesyl-directing CaaX box (CTLM) (24), while the other cysteine (106) is a potential site for palmitoylation (35). In *S. cerevisiae*, substitution of serine for cysteine at position 106 or 107 resulted in failure of Gβγ to bind to the plasma membrane (35). The Cys 107 substitution also resulted in reduced steady-state levels of Ste18p, suggesting that Cys 107 farnesylation is required for Ste18p stability (35). Furthermore, previous genetic studies (30, 78) have demonstrated that yeast mutants with substitutions at either cysteine residue are unresponsive to pheromone. Further experimentation is needed to determine the importance of these two conserved cysteine residues to GNG-1 function in *N. crassa*.

The intron-exon boundaries and mRNA splicing patterns for several mammalian Gγ-subunit genes have already been characterized (19, 20, 25, 28, 52). In all cases, the 5′-untranslated region of the mRNA contains one intron. A second intron is located in the ORF, and its position relative to the amino acid sequence is conserved between the Gγ-subunit genes (20). The *S. cerevisiae STE18* ORF does not contain an intron (http://www.yeastgenome.org). In contrast, both *S. pombe git11* (http://www.genedb.org/genedb/pombe/index.jsp) and *N. crassa gng-1* have introns in their ORFs. However, there are no reports of introns in the 5′ UTRs of *STE18* and *git11*. In this study, we have identified two introns in *N. crassa gng-1* at positions that correspond to those found in mammalian Gγ-subunit genes. We previously reported a similar phenomenon with respect to conserved intron positions in mammalian and *N. crassa* Gα genes (68). The remarkable conservation of intron positions between mammalian and *N. crassa* Gγ (and Gα) genes suggests that these sequences play a regulatory role in mRNA synthesis or stability. Future studies will investigate these possibilities.

The Δ*gng-1* mutant displays phenotypes identical to those observed in Δ*gnb-1* strains (44, 80), and the Δ*gnb-1* Δ*gng-1* double mutant is indistinguishable from either single mutant. Our results also demonstrate that loss of *gng-1* or *gnb-1* results in a significant reduction in GNB-1 or GNG-1 protein levels, respectively, from plasma membrane fractions (Fig. 2E), suggesting interdependence between GNB-1 and GNG-1 for their stability in vivo. This is similar to the situation of *S. cerevisiae*, in which Ste18p is barely detectable in *ste4* mutants while Ste4p is reduced only 50% in *ste18* cells (34). Taken together, our data support the hypothesis that GNB-1 and GNG-1 regulate identical events in *N. crassa* and form an active Gβγ complex in vivo. The finding that GNB-1 is coprecipitated with GNG-1 using an antibody directed against an epitope on GNG-1 provides strong evidence for a direct, physical association between these two proteins in vivo.

Like Δ*gnb-1* mutants (80), Δ*gng*-1 strains have lower levels of Gα proteins than the wild type. This is in contrast to results reported for *S. cerevisiae*, where Gpa1p is present at normal levels and is localized to the plasma membrane in the absence of Gβγ (64). The major effect caused by loss of the Gβγ dimer in *N. crassa* appears posttranscriptional, because normal or appreciable levels of *gna-1*, *gna-2*, and *gna-3* transcripts are produced in Δ*gng-1* and Δ*gnb-1* strains. In contrast, deletion of a single Gα does not greatly influence GNB-1 levels (38, 41, 43); a significant reduction in GNB-1 amount is only observed in a mutant lacking both GNA-1 and GNA-3 or all three Gα proteins (43). This finding suggests that the absence of multiple Gα proteins can influence the amount of Gβγ dimer anchored to the plasma membrane of *N. crassa*.

Many of the defects shared by Δ*gnb-1* and Δ*gng-1* strains can be explained by reduced amounts of Gα proteins. The female sterility of these mutants is similar to that of Δ*gna-1* and Δ*gna-1* Δ*gna-2* mutants (37, 44). These strains are defective in trichogyne attraction toward the male cell and form small aberrant perithecia with no ascospores after fertilization (37, 80). In contrast to GNA-1 and GNA-2, GNA-3 levels in submerged cultures were not greatly reduced (30 to 50%), suggesting that the Gβγ subunit is not crucial for GNA-3 stability in vegetative hyphal tissue. However, GNA-3 levels are significantly reduced in VM and SCM plate cultures. Based just on protein amount, it is not easy to predict the phenotypic outcome of lower GNA-3 levels in the various tissues. It is possible

that GNA-3 is coupled to different receptors, and thus its turnover might be regulated differently in various cell types. On the other hand, GNB-1 may act as a direct regulator of downstream effectors, while GNA-3 is only required to regulate GNB-1 function. Such a scenario has been described for *S. cerevisiae*, where Gpa1p negatively regulates Ste4p function during pheromone signal transduction (18, 65, 81).

It was demonstrated previously that Δ*gnb-1* strains have low levels of intracellular cAMP when cultured on solid medium but normal amounts of cAMP in submerged culture (80). We have obtained similar results with Δ*gng-1* mutants (Table 3). The Δ*gng-1* mutant conidiates abundantly on solid medium and in submerged cultures, and phenotypically it resembles Δ*gna-1*, Δ*gna-1* Δ*gna-2*, and Δ*gna-3* mutants. It was hypothesized that the smaller amount of GNA-1 and GNA-2 in Δ*gnb-1* mutants is responsible for the reduction in cAMP levels (80). This hypothesis is supported by results from previous studies with both Δ*gna-1* deletion and *gna-1* constitutively activated alleles (38, 39, 79). The observation of normal cAMP levels in submerged cultures of Δ*gnb-1* and Δ*gng-1* strains is similar to results determined for Δ*gna-1* and Δ*gna-1* Δ*gna-2* mutants (38). In contrast, submerged liquid cultures of Δ*gna-3* mutants produce low levels of intracellular cAMP, presumably due to reduced amounts of adenylyl cyclase protein (41). Tissue-specific effects on cAMP metabolism due to loss of a Gγ-subunit gene have also been observed in mice, where the $G\gamma_7$ protein regulates adenylyl cyclase activity in specific regions of the brain (61).

Some phenotypes observed in Δ*gnb-1* mutants cannot be explained by low levels of Gα proteins. For example, Δ*gnb-1* mutants have essentially normal apical extension rates on various media (80), while a mutant lacking all three Gα proteins exhibits severely restricted growth (43). A possible explanation is that although Gα protein amounts are reduced in Δ*gnb-1* (and Δ*gng-1)* mutants, free Gα proteins, untethered by GNB-1, can regulate downstream effectors. A similar model for G-protein functional interactions has been suggested for *S. pombe*, where Gpa2 remains partially active during cAMP signaling in *git5* (Gβ) mutants (45).

In this study, we provide evidence that GNG-1 is the sole Gγ subunit in *N. crassa* and that this protein forms a physical association with the only Gβ protein, GNB-1. Levels of GNG-1 and GNB-1 are decreased in the absence of the other subunit, consistent with decreased protein stability. The GNB-1/GNG-1 Gβγ heterodimer acts as a unit during signaling, with loss of either protein leading to similar defects, including a severe reduction in Gα protein levels. Future studies will focus on elucidation of the mechanism whereby loss of GNG-1 leads to smaller amounts of GNB-1 and the three Gα proteins and on understanding the contribution of individual G protein subunits to regulation of downstream effectors in *N. crassa*.

ACKNOWLEDGMENTS

We thank Brianna Rider for assistance with DNA subcloning and Southern and Northern analyses, Sheven Poole for isolation of the hβJ strain, Ann Kays for construction of the *his-3*a strain, and Hyojeong Kim and Suzanne Philips for comments on the manuscript and helpful discussions.

This work was supported by Public Health Service grant GM48626 from the National Institutes of Health (to K.A.B.).

REFERENCES

1. **Altschul, S. F., T. L. Madden, A. A. Schäffer, J. Zhang, W. Miller, and D. J. Lipman.** 1997. Gapped BLAST and PSI-BLAST: a new generation of protein database search programs. Nucleic Acids Res. **25:**3389–3492.
2. **Aramayo, R.** 1996. Gene replacement at the *his-3* locus of *Neurospora crassa*. Fungal Genet. Newsl. **43:**9–13.
3. **Baasiri, R. A., X. Lu, P. S. Rowley, G. E. Turner, and K. A. Borkovich.** 1997. Overlapping functions for two G protein α subunits in *Neurospora crassa*. Genetics **147:**137–145.
4. **Baxevanis, A. D., and D. Landsman.** 1995. The HMG-1 box protein family: classification and functional relationship. Nucleic Acids Res. **23:**1604–1613.
5. **Bell-Pedersen, D., J. C. Dunlap, and J. J. Loros.** 1996. Distinct *cis*-acting elements mediate clock, light, and developmental regulation of the *Neurospora crassa eas* (*ccg-2*) gene. Mol. Cell. Biol. **16:**513–521.
6. **Birnbaumer, L.** 1992. Receptor to effector signaling through G proteins: roles for βγ dimers as well as α subunits. Cell **71:**1069–1072.
8. **Bistis, G. N.** 1981. Chemotropic interactions between trichognes and conidia of opposite mating-type in *Neurospora crassa*. Mycologia **73:**959–975.
9. **Bistis, G. N.** 1983. Evidence of difusible, mating-type-specific trichogyne attractants in *Neurospora crassa*. Exp. Mycol. **7:**292–295.
10. **Blumer, K. J., and J. Thorner.** 1990. β And γ subunits of a yeast guanine nucleotide-binding protein are not essential for membrane association for receptor coupling. Proc. Natl. Acad. Sci. USA **87:**4363–4367.
11. **Bowman, E. J., and B. J. Bowman.** 1988. Purification of vacuolar membranes, mitochondria, and plasma membranes from Neurospora crassa and modes of discriminating among the different H+ ATPases. Methods Enzymol. **157:** 562–573.
7. **Brizzard, B. L., R. G. Chubet, and D. L. Vizard.** 1994. Immunoaffinity purification of FLAG epitope-tagged bacterial alkaline phosphatase using a novel monoclonal antibody and peptide elution. BioTechniques **16:**730–735.
12. **Cabrera-Vera, T. M., J. Vanhauwe, T. O. Thomas, M. Medkova, A. Preininger, M. R. Mazzoni, and H. E. Hamm.** 2003. Insight into G protein structure, function, and regulation. Endocrine Res. **24:**765–781.
13. **Case, M. E., M. Schweizer, S. R. Kushner, and N. H. Giles.** 1979. Efficient transformation of *Neurospora crassa* by utilizing hybrid plasmid DNA. Proc. Natl. Acad. Sci. USA **76:**5259–5263.
14. **Clapham, D. E., and E. J. Neer.** 1997. G protein beta gamma subunit. Annu. Rev. Pharmacol. Toxicol. **37:**167–203.
15. **Clark, K. L., D. Dignard, D. Y. Thomas, and M. Whiteway.** 1993. Interactions among the subunits of the G protein involved in *Saccharomyces cerevisiae* mating. Mol. Cell. Biol. **13:**1–8.
16. **Davis, R. H., and F. J. de Serres.** 1970. Genetic and microbiological research techniques in *Neurospora crassa*. Methods Enzymol. **71A:**79–143.
17. **Dohlman, H. G.** 2002. G proteins and pheromone signaling. Annu. Rev. Physiol. **64:**129–152.
18. **Dowell, S. J., A. L. Bishop, S. L. Dyos, A. J. Brown, and M. S. Whiteway.** 1998. Mapping of a yeast G protein βγ signaling interaction. Genetics **150:** 1407–1417.
19. **Downes, G. B., N. G. Copeland, N. A. Jenkins, and N. Gautam.** 1998. Structure and mapping of the G protein gamma 3 subunit gene and a divergently transcribed novel gene, gng3lg. Genomics **53:**220–230.
20. **Downes, G. B., and N. Gautam.** 1999. The G protein subunit gene families. Genomics **62:**544–552.
21. **Ebbole, D., and M. S. Sachs.** 1990. A rapid and simple method for isolation of *Neurospora crassa* homokaryons using microconidia. Fungal Genet. Newsl. **37:**17–18.
22. **Elion, E. A.** 2000. Pheromone response, mating and cell biology. Curr. Opin. Microbiol. **3:**1210–1215.
23. **Evanko, D. S., M. M. Thiyagarajan, D. P. Siderovski, and P. B. Wedegaertner.** 2001. G beta gamma isoforms selectively rescue plasma membrane localization and palmitoylation of mutant Galphas and Galphaq. J. Biol. Chem. **276:**23945–23953.
24. **Finegold, A. A., W. R. Schafer, J. Rine, M. Whiteway, and F. Tamanoi.** 1990. Common modifications of trimeric G proteins and ras protein: involvement of polyisoprenylation. Science **249:**165–169.
25. **Fischer, K. J., and N. N. Aronson, Jr.** 1992. Characterization of the cDNA and genomic sequence of a G protein γ subunit (γ5). Mol. Cell. Biol. 12:1585–1591.
26. **Folco, H. D., M. Freitag, A. Ramon, E. D. Temporini, M. E. Alvarez, I. Garcia, C. Scazzocchio, E. U. Selker, and A. L. Rosa.** 2003. Histone H1 is required for proper regulation of pyruvate decarboxylase gene expression in *Neurospora crassa*. Eukaryot. Cell **2:**341–350.
27. **Galagan, J. E., K. A. Borkovich, E. Selker, N. D. Read, D. Jaffe, et al.** 2003. The genome sequence of the filamentous fungus *Neurospora crassa*. Nature **422:**859–868.
28. **Gautam, N., G. B. Downes, K. Yan, and O. Kisselev.** 1998. The G-protein βγ complex. Cell Signal. **10:**447–455.
29. **Griffiths, A. J. F.** 1982. Null mutants of the A and a mating type alleles of *Neurospora crassa*. Can. J. Genet. Cytol. **24:**167–176.
30. **Grishin, A. V., J. L. Weiner, and K. J. Blumer.** 1994. Biochemical and genetic

analysis of dominant-negative mutations affecting a yeast G-protein γ subunit. Mol. Cell. Biol. **14:**4571–4578.
31. **Gurr, S. J., S. E. Unkles, and J. R. Kinghorn.** 1987. The structure and organization of nuclear genes in filamentous fungi, p. 93–139. *In* J. R. Kinghorn (ed.), Gene structure in eukaryotic microbes, vol. 22. IRL Press Ltd., Oxford, United Kingdom.
32. **Hamm, H. E.** 1998. Many faces of G protein signaling. J. Biol. Chem. **273:**669–672.
33. **Hanahan, D.** 1983. Studies of transformation of *Escherichia coli* with plasmids. J. Mol. Biol. **166:**557.
34. **Hirschman, J. E., G. S. De Zutter, W. F. Simonds, and D. D. Jenness.** 1997. The βγ complex of the yeast pheromone response pathway. J. Biol. Chem. **272:**240–248.
35. **Hirschman, J. E., and D. D. Jenness.** 1999. Dual lipid modification of the yeast Gγ subunit Ste18p determine membrane localization of Gβγ. Mol. Cell. Biol. **19:**7705–7711.
36. **Iniguez-Lluhi, J. A., M. I. Simon, J. D. Robishaw, and A. G. Gilman.** 1992. G protein beta gamma subunits synthesized in Sf9 cells. Functional characterization and the significance of prenylation of gamma. J. Biol. Chem. **267:**23409–23417.
37. **Ivey, F. D., P. Hodge, G. E. Turner, and K. A. Borkovich.** 1996. The Gαi homologue *gna-1* controls multiple differentiation pathways in *Neurospora crassa*. Mol. Cell. Biol. **7:**1283–1297.
38. **Ivey, F. D., Q. Yang, and K. A. Borkovich.** 1999. Positive regulation of adenylyl cyclase activity by Gαi homologue in *Neurospora crassa*. Fungal Genet. Biol. **26:**48–61.
39. **Ivey, F. D., A. M. Kays, and K. A. Borkovich.** 2002. Shared and independent roles for a Galpha(i) protein and adenylyl cyclase in regulating development and stress response in *Neurospora crassa*. Eukaryot. Cell **1:**634–642.
40. **Kasahara, S., P. Wang, and D. L. Nuss.** 2000. Identification of *bdm-1*, a gene involved in G protein β-subunit function and α-subunit accumulation. Proc. Natl. Acad. Sci. USA **97:**412–417.
41. **Kays, A. M., P. S. Rowley, R. A. Baasiri, and K. A. Borkovich.** 2000. Regulation of conidiation and adenylyl cyclase levels by the Gα protein GNA-3 in *Neurospora crassa*. Mol. Cell. Biol. **20:**7693–7705.
42. **Kays, A. M., and K. A. Borkovich.** 2004. Signal transduction pathways mediated by heterotrimeric G proteins, p. 175–207. *In* R. Bramble and G. A. Marzluf (ed.), The mycota III, biochemistry and molecular biology, 2nd ed. Springer-Verlag, Berlin-Heidelberg, Germany.
43. **Kays, A. M., and K. A. Borkovich.** 2004. Severe impairment of growth and differentiation in a *Neurospora crassa* mutant lacking all heterotrimeric Gα proteins. Genetics **167:**1229–1240.
44. **Kim, H., and K. A. Borkovich.** 2004. A pheromone receptor gene, pre-1, is essential for mating type-specific directional growth and fusion of trichogyne and female fertility in *Neurospora crassa*. Mol. Microbiol. **52:**1781–1798.
45. **Landry, S., and C. S. Hoffman.** 2001. The git5 Gβ form an apical Gβγ dimer acting in the fission yeast glucose/cAMP pathway. Genetics **157:**1159–1168.
46. **Lim, W. K., C. S. Myung, J. C. Garrison, and R. R. Neubig.** 2001. Receptor-G protein gamma specificity: gamma11 shows unique potency for A(1) adenosine and 5-HT(1A) receptors. Biochemistry **40:**10532–10541.
47. **Lodowski, D. T., J. A. Pitcher, W. D. Capel, R. J. Lefkowitz, and J. J. Tesmer.** 2003. Keeping G proteins at bay: a complex between G protein-coupled receptor kinase 2 and Gbetagamma. Science **300:**1256–1262.
48. **Maltese, W. A., and J. D. Robishaw.** 1990. Isoprenylation of C-terminal cysteine in a G-protein gamma subunit. J. Biol. Chem. **265:**18071–18074.
49. **Mason, M. G., and J. R. Botella.** 2001. Isolation of a novel G-protein gamma-subunit from *Arabidopsis thaliana* and its interaction with Gbeta. Biochim. Biophys. Acta **1520:**147–153.
50. **Neves, S. R., P. T. Ram, and R. Iyengar.** 2002. G protein pathways. Science **296:**1636–1639.
51. **Nishimura, M., G. Park, and J. R. Xu.** 2003. The G-beta subunit MGB1 is involved in regulating multiple steps of infection-related morphogenesis in *Magnaporthe grisea*. Mol. Microbiol. **50:**231–243.
52. **Ong, O. C., K. Hu, H. Rong, R. H. Lee, and B. K. Fung.** 1997. Gene structure and chromosome localization of the Gγc subunit of human cone G-protein (GNGT2). Genomics **44:**101–109.
53. **Pall, M. L., and J. P. Brunelli.** 1994. New plasmid and lambda/plasmid hybrid vectors and *Neurospora crassa* genomic library containing the *bar* selectable marker and the Cre/*lox* site-specific recombination for use in filamentous fungi. Fungal Genet. Newsl. **41:**63–65.
54. **Plesofsky-Vig, N., D. Light, and R. Brambl.** 1983. Paedogenetic conidiation in *Neurospora crassa*. Exp. Mycol. **7:**283–286.
55. **Raju, N. B.** 1992. Genetic control of the sexual cycle in *Neurospora.* Mycol. Res. **96:**241–262.
56. **Rosen, S. J., H. Yu, and T. H. Adams.** 1999. The *Aspergillus nidulans* sfaD gene encodes a G protein beta subunit that is required for normal growth and repression of sporulation. EMBO J. **18:**5592–5600.
57. **Sambrook, J., and D. W. Russel.** 2001. Molecular cloning: a laboratory manual. Cold Spring Harbor Laboratory Press, Cold Spring Harbor, N.Y.
58. **Simonds, W. F., B. J. E. Butrynski, N. Gautam, G. Unson, and A. M. Spiegel.** 1991. G-Protein βγ dimers. Membrane targeting requires subunit coexpression and intact gamma C-A-A-X domain. J. Biol. Chem. **266:**5363–5366.
59. **Sinensky, M.** 2000. Recent advances in the study of prenylated proteins. Biochim. Biophys. Acta **1484:**93–106.
60. **Schmidt, C. J., T. C. Thomas, M. A. Levine, and E. J. Neer.** 1991. Specificity of G-protein β and γ subunit interaction. J. Biol. Chem. **267:**13807–13810.
61. **Schwindinger, W. F., K. S. Betz, K. E. Giger, A. Sabol, S. K. Bronson, and J. D. Robishaw.** 2003. Loss of G protein γ7 alters behavior and reduces striatal α(olf) level and cAMP production. J. Biol. Chem. **278:**6575–6579.
62. **Schwindinger, W. F., K. E. Giger, K. S. Betz, A. M. Stauffer, E. M. Sunderlin, L. J. Sim-Selley, D. E. Selley, S. K. Bronson, and J. D. Robishaw.** 2004. Mice with deficiency of G protein γ3 are lean and have seizures. Mol. Cell. Biol. **24:**7758–7768.
63. **Sondek, J., A. Bohm, D. G. Lambright, H. E. Hamm, and P. B. Sigler.** 1996. Crystal structure of a G-protein βγ dimmer at 2.1 Å resolution. Nature **379:**369–374.
64. **Song, J. P., and H. G. Dohlman.** 1996. Partial constitutive activation of pheromone responses by palmitoylation-site mutant of a G protein α subunit in yeast. Biochemistry **35:**14806–14817.
65. **Spain, B. H., D. Koo, M. Ramakrishnan, B. Dzudzor, and J. Colicelli.** 1995. Truncated forms of a novel yeast protein suppress the lethality of a G protein alpha subunit deficiency by interacting with the beta subunit. J. Biol. Chem. **270:**25435–25444.
66. **Staben, C., B. Jensen, M. Singer, J. Pollock, M. Schechtman, J. Kinsey, and E. Selker.** 1989. Use of a bacterial hygromycin B resistance gene as a dominant selectable marker in *Neurospora crassa* transformation. Fungal Genet. Newsl. **36:**79–81.
67. **That, T. C., and G. Turian.** 1978. Ultrastructural study of microcyclic macroconidiation in *Neurospora crassa*. Arch. Microbiol. **116:**279–288.
68. **Turner, G. E., and K. A. Borkovich.** 1993. Identification of a G protein α subunit from *Neurospora crassa* that is a member of Gi family. J. Biol. Chem. **268:**14805–14811.
69. **Vann, D. C.** 1995. Electroporation-based transformation of freshly harvested conidia of *Neurospora crassa*. Fungal Genet. Newsl. **42A:**53.
70. **Vogel, H. J.** 1964. Distribution of lysine pathways among fungi: evolutionary implications. Am. Nat. **98:**435–446.
71. **Wang, Q., B. K. Mullah, and J. D. Robishaw.** 1999. Ribozyme approach identifies a functional association between the G protein β_1g_7 subunits in the β-adrenergic receptor signaling pathway. J. Biol. Chem. **274:**17365–17371.
72. **Wang, P., J. R. Perfect, and J. Heitman.** 2000. The G-protein beta subunit GPB1 is required for mating and haploid fruiting in *Cryptococcus neoformans*. Mol. Cell. Biol. **20:**352–362.
73. **Welton, R. M., and C. S. Hoffman.** 2000. Glucose monitoring in fission yeast via gpa2 Gα, the git5 Gβ and the git3 putative glucose receptor. Genetics **156:**513–521.
74. **Westergaard, M., and H. K. Mitchell.** 1947. Neurospora V. A synthetic medium favoring sexual reproduction. Am. J. Bot. **34:**573–577.
75. **White, R. J., P. W. Rigby, and S. P. Jackson.** 1992. The TATA-binding protein is a general transcription factor for RNA polymerase. J. Cell Sci. Suppl. **16:**1–7.
76. **Whiteway, M., L. Hougan, D. Dignard, D. Y. Thomas, L. Bell, G. C. Saari, F. J. Grant, P. O'Hara, and V. MacKay.** 1989. The *STE4* and *STE18* genes of yeast encode potential β and γ subunits of the mating factor receptor-coupled G protein. Cell **56:**476–477.
77. **Whiteway, M., D. Dignard, and D. Y. Thomas.** 1992. Mutagenesis of Ste18, a putative G gamma subunit in the *Saccharomyces cerevisiae* pheromone response pathway. Biochem. Cell Biol. **70:**1230–1237.
78. **Whiteway, M. S., and D. Y. Thomas.** 1994. Site-directed mutations altering the CAAX box of Ste18, the yeast pheromone-response pathway G gamma subunit. Genetics **137:**967–976.
79. **Yang, Q., and K. A. Borkovich.** 1999. Mutational activation of a Gαi causes uncontrolled proliferation of aerial hyphae and increased sensitivity to heat and oxidative stress in *Neurospora crassa*. Genetics **151:**107–117.
80. **Yang, Q., S. I. Poole, and K. A. Borkovich.** 2002. A G-protein β subunit required for sexual and vegetative development and maintenance of normal Gα protein levels in *Neurospora crassa*. Eukaryot. Cell **1:**378–390.
81. **Zhang, M., and D. J. Tipper.** 1993. Suppression of a dominant G-protein beta-subunit mutation in yeast by G alpha protein expression. Mol. Microbiol. **9:**813–821.
82. **Zhang, S., O. A. Coso, C. Lee, J. S. Gutkind, and W. F. Simonds.** 1996. Selective activation of effector pathways brain specific G protein β5. J. Biol. Chem. **271:**33575–33579.
83. **Zhang, N., Y. Long, and P. N. Devreotes.** 2001. Gγ in *Dictyostelium*: its role in localization of Gβγ to the membrane is required for chemotaxis in shallow gradients. Mol. Biol. Cell. **12:**3204–3213.